

## Ultrafast Coherent Generation of Hot Electrons Studied via Band-to-Acceptor Luminescence in GaAs

Alfred Leitenstorfer, Andrea Lohner, and Thomas Elsaesser\*

*Physik Department E 11, Technische Universität München,  
D-85748 Garching, Germany*

Stefan Haas and Fausto Rossi

*Fachbereich Physik, Philipps-Universität Marburg,  
D-35032 Marburg, Germany*

Tilmann Kuhn

*Institut für Theoretische Physik, Universität Stuttgart,  
D-70505 Stuttgart, Germany*

W. Klein, G. Boehm, G. Traenkle, and G. Weimann

*Walter-Schottky-Institut, Technische Universität München,  
D-85748 Garching, Germany*

(Received 8 March 1994)

The distribution of hot electrons excited with femtosecond laser pulses is studied via spectrally resolved band-to-acceptor luminescence. Our data demonstrate for the first time that the coherent coupling between the laser pulse and the interband polarization strongly influences the initial carrier distribution. The energetic width of carrier generation is broadened due to rapid phase-breaking scattering events. Theoretical results from a Monte Carlo solution of the semiconductor Bloch equations including on the same kinetic level coherent and incoherent phenomena, are in excellent agreement with the experimental data.

PACS numbers: 72.10.Di, 72.80.Ey, 78.47.+p

The nonequilibrium behavior of carriers in semiconductors is governed by the strong coupling of different elementary excitations. Optical excitation of interband transitions results in an ultrafast electron-hole dynamics which is influenced by both coherent and incoherent phenomena. The thermalization of a photogenerated electron-hole plasma to quasi-Fermi distributions has extensively been studied by ultrafast spectroscopy monitoring transient absorption or luminescence spectra [1–3]. The incoherent dynamics of hot electrons has been investigated via band-to-acceptor luminescence that is due to recombination of electrons created by continuous wave, picosecond, or femtosecond excitation with holes bound to acceptor atoms [4–9]. In such experiments, the substantial width of the acceptor wave function in  $\mathbf{k}$  space and the time-independent hole distribution allow a selective observation of the electron dynamics, even at energies high above the band gap and for excitation densities as low as  $10^{13} \text{ cm}^{-3}$ . In this regime, the emission spectra show a series of well-defined peaks which are related to the nonequilibrium electron distribution. Band-structure parameters, electron-phonon scattering rates, and—for higher densities—carrier-carrier scattering rates have been deduced from the experimental data.

Most of the experiments on thermalization have been interpreted in terms of a fully incoherent carrier dynamics where carrier-carrier ( $cc$ ) and carrier-phonon ( $cp$ ) scattering lead to a rapid redistribution of electrons and/or

holes. These phenomena have been modeled by ensemble Monte Carlo (EMC) simulations based on the semiclassical Boltzmann transport theory. On the other hand, it is well known that photoexcitation with coherent light induces a coherent polarization in the carrier system. The dynamics of this polarization and its decay by phase relaxation have mainly been studied in four-wave-mixing [10,11] and hole-burning [12] experiments where, however, only indirect information on the transient carrier distributions is obtained. In contrast, the investigation of the band-to-acceptor luminescence should provide much more specific information on the initial distribution of electrons and its temporal evolution.

In this Letter, we provide for the first time direct experimental evidence that the nonequilibrium electron distributions created by femtosecond excitation of GaAs are strongly influenced by the coherent nature of light-matter interaction. The dephasing processes result in a density dependent broadening of the photogenerated nonequilibrium distribution which cannot be explained in terms of semiclassical transport theory. Luminescence profiles for excitation densities between  $5 \times 10^{13}$  and  $5 \times 10^{16} \text{ cm}^{-3}$  give direct insight into these phenomena which are analyzed by means of detailed simulations based on a generalized Monte Carlo solution of the semiconductor Bloch equations (SBE) [13,14].

In our experiment, a  $3 \mu\text{m}$  thick  $p$ -type GaAs layer grown by molecular beam epitaxy is studied at a lattice

temperature of  $T_L = 10$  K. The sample doped with Be acceptors of a binding energy of 28 meV [15] and a concentration of  $3 \times 10^{16} \text{ cm}^{-3}$  [16] is excited at a photon energy of 1.73 eV by transform-limited 150 fs pulses from a mode-locked Ti:sapphire laser. Time-integrated luminescence spectra are recorded with a double monochromator (spectral resolution 1 meV) and a single-photon-counting multiplier. The excitation densities given below are estimated from the spot size of the laser beam on the sample, the penetration depth, and the number of photons absorbed per pulse.

Excitation of the heavy hole to conduction band transition at 1.73 eV creates electrons and (free) holes with respective excess energies of  $E_e = 185$  meV and  $E_{hh} = 25$  meV [17]. The dynamics of the photoexcited electrons is monitored via the band-to-acceptor luminescence which is red shifted with respect to the laser pulse. In Figs. 1(a)–1(d), we present emission spectra for four different excitation densities between  $8 \times 10^{13}$  and  $2 \times 10^{16} \text{ cm}^{-3}$ . The spectra at low carrier density exhibit a first peak around 1.68 eV which originates from the re-

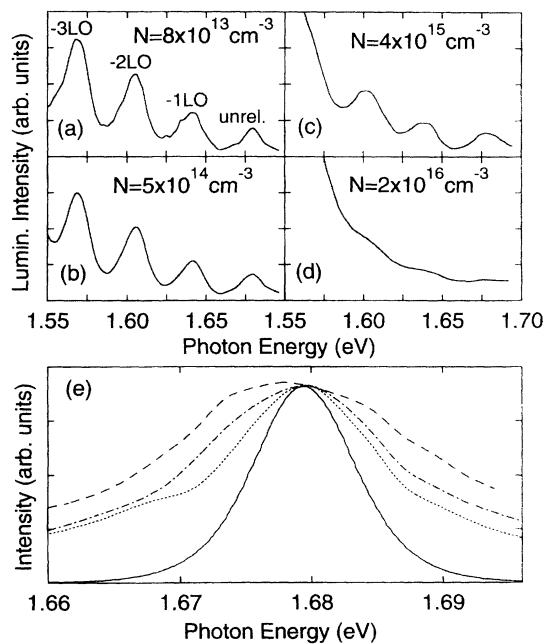


FIG. 1. (a)–(d) Hot electron luminescence spectra of GaAs (lattice temperature  $T_L = 10$  K) measured for different excitation densities  $N$ . The intensity of band-to-acceptor emission is plotted versus photon energy. The spectra show a first peak (unrel.) that originates from conduction band states optically coupled by the excitation pulse (photon energy 1.73 eV, pulse duration 150 fs) and a series of phonon replicas. Within the experimental accuracy, the lines exhibit an identical spectral width and broaden with increasing carrier concentration. (e) Spectral profile of the first luminescence peak for carrier densities of  $N = 8 \times 10^{13} \text{ cm}^{-3}$  (dotted line),  $5 \times 10^{14} \text{ cm}^{-3}$  (dash-dotted line), and  $4 \times 10^{15} \text{ cm}^{-3}$  (dashed line). For comparison, the spectral envelope of the laser pulses is shown (shifted to lower photon energy by 50 meV, solid line).

combination of electrons from states optically coupled to the valence band by the laser excitation, and—at lower photon energy—a series of phonon replicas. The latter are due to electrons which have emitted one, two, or three longitudinal-optical (LO) phonons and reflect the carrier dynamics at later times. The intensity of the phonon replicas increases with decreasing photon energy mainly because of the rising matrix element of the band-to-acceptor transition [18]. For a very low excitation density of  $N = 8 \times 10^{13} \text{ cm}^{-3}$ , the individual emission lines have an identical spectral width of 17 meV. With increasing carrier concentration, the first peak and the phonon replicas broaden substantially, resulting in a structureless luminescence spectrum for  $N > 2 \times 10^{16} \text{ cm}^{-3}$ .

The spectral profile of the first peak was studied in detail. In Fig. 1(e), this part of the spectrum is plotted for the three carrier concentrations on an extended energy scale and compared to the (red shifted) spectral profile of the laser pulses (solid line). Even for the very low excitation density of  $N = 8 \times 10^{13} \text{ cm}^{-3}$ , the spectral width of 17 meV (FWHM) is considerably higher than the pulse width of about 10 meV. In Fig. 2(a), the linewidth

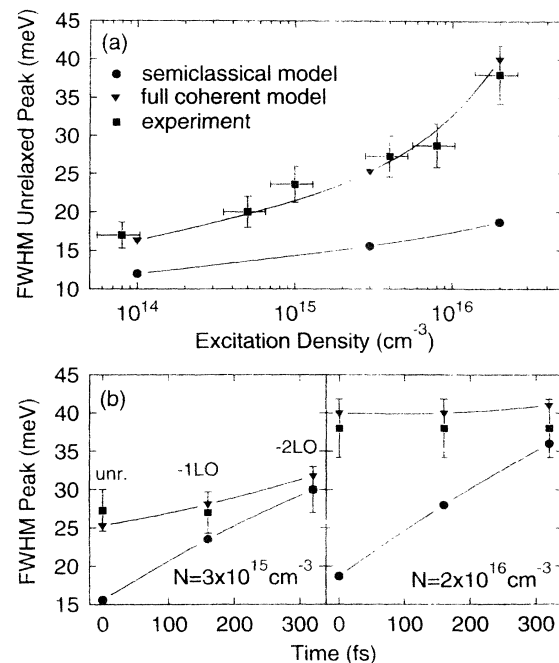


FIG. 2. (a) Spectral FWHM of the first luminescence peak (unrel.) as a function of excitation density. The data (squares) are compared to theoretical values calculated from a simulation including the coherent coupling of laser field and polarization in the sample (triangles) and from a semiclassical model of the incoherent carrier dynamics (circles). (b) Spectral width of the first, second ( $-1\text{LO}$ ), and third ( $-2\text{LO}$ ) luminescence peak for excitation densities of  $3 \times 10^{15} \text{ cm}^{-3}$  (left hand side) and  $2 \times 10^{16} \text{ cm}^{-3}$  (right hand side). The data showing an identical width of the peaks (squares) are compared to results from the two theoretical models (circles and triangles). The time scale was calculated with an LO phonon emission time of 160 fs.

is plotted as a function of  $N$  (squares), showing a strong increase from 17 meV at  $N = 8 \times 10^{13} \text{ cm}^{-3}$  to approximately 40 meV at  $N = 2 \times 10^{16} \text{ cm}^{-3}$  [19].

In Fig. 2(b), the spectral width of the first three luminescence peaks which are separated in time by a single LO phonon emission time  $\tau_{\text{LO}} = 160 \text{ fs}$ , is plotted for two excitation densities (squares). At each density, the first ("unrelaxed") peak exhibits almost the same spectral width as the phonon replicas occurring at later times.

The pulse duration of 150 fs is slightly shorter than the single LO phonon emission time of  $\tau_{\text{LO}} = 160 \text{ fs}$ . For carrier concentrations below  $10^{15} \text{ cm}^{-3}$ , the thermalization of the photoexcited carriers to a Fermi-like distribution takes much longer than  $\tau_{\text{LO}}$ . Thus, within the first LO phonon emission time, most of the generated electrons are part of the nonequilibrium distribution giving rise to the first luminescence peak at 1.68 eV. This initial electron distribution is analogous to that studied in femtosecond time-resolved luminescence measurements [3], but completely different from the nonequilibrium population generated by picosecond or continuous wave excitation in a quasistationary way. In the latter case, the photogeneration rate of carriers is much lower than the intraband redistribution rates. Consequently, the majority of electrons form a Fermi distribution at the bottom of the conduction band, and the few electrons populating the directly excited states at high excess energy interact with this cold distribution.

We now discuss the photogeneration process in order to understand the shape and the density dependence of the spectra. Within the semiclassical description, the laser pulse generates an initial nonequilibrium distribution of an energy broadening that is determined by the spectral width of the pulse and by band-structure details like heavy-hole warping. The subsequent emission of LO phonons leads to the formation of replicas of the excitation peak. At higher densities, carrier-carrier scattering results in a broadening that increases with time. Thus, replicas at lower energies should exhibit a width larger than those at higher energies and—in particular—larger than the unrelaxed peak. The spectra calculated with a conventional (semiclassical) EMC simulation including both  $cc$  and  $cp$  scattering are presented in Figs. 3(a)–3(c) and show exactly this behavior. The width of the calculated luminescence peaks plotted in Fig. 2(b) (circles) exhibits a well-pronounced increase which remains true even if more refined models of scattering rates, e.g., dynamical screening, or band structure, e.g., warping, are considered.

On the contrary, our luminescence spectra for excitation densities below  $10^{15} \text{ cm}^{-3}$  (Fig. 1) exhibit a spectral width of the first emission peak of 17 to 25 meV, significantly higher than the bandwidth of the 150 fs laser pulses of 10 meV. For this large excitation bandwidth, the inhomogeneous broadening due to warping of the valence band cannot account for the excess linewidth and for a

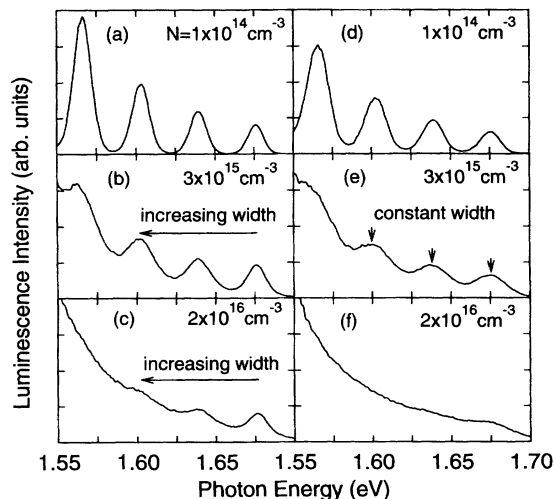


FIG. 3. Luminescence spectra calculated from the simulations (a)–(c) of the semiclassical Boltzmann equation and (d)–(f) of the semiconductor Bloch equations for various excitation densities  $N$  (same parameters as in the experiment).

density-dependent width at low carrier concentrations  $N$ . For  $N \approx 10^{14} \text{ cm}^{-3}$ , the experimental results and the theoretical simulations in Ref. [7] give  $cc$  scattering rates much too low to account for our results. Furthermore, our data for *all* excitation densities show a nearly constant linewidth of the different peaks, in sharp contrast to the results of the semiclassical model of carrier dynamics [Fig. 2(b)].

The interaction of a semiconductor with a short laser pulse is a coherent phenomenon as is well known from four-wave-mixing experiments. This fact, however, is usually neglected in the analysis of luminescence experiments. The profile of the first luminescence peak observed in our measurements is strongly influenced by this coherent nature of the carrier generation process. During excitation, the coherent coupling of the laser pulse with the polarization of the sample gives rise to a nonequilibrium electron distribution that covers a substantially wider energy interval than the spectrum of the transform-limited laser pulse. In this regime, the spectral width of the carrier generation rate is determined by a momentary spectral width which corresponds to the inverse of the time elapsed after the onset of the pulse (cf. Fig. 1 of Ref. [14]). For an idealized system with dephasing times much longer than the pulse duration, the generation rate contains negative contributions at later times, i.e., coherent off-resonance recombinations, leading to a carrier distribution defined by the pulse spectrum. During the pulse, however, phase-breaking scattering events destroy the coherence, suppress this recombination off-resonance, and result in a width of the distribution which is larger than the energetic width of the laser pulse and which increases with carrier density. The measured nearly con-

stant linewidth of the initial peak and of the various replicas for a given carrier density is a clear consequence of the fact that the broadening is mainly introduced by the carrier generation while the subsequent broadening due to incoherent scattering processes is of minor importance. Thus, *the emission spectra give direct evidence of the coherent nature of the carrier generation process.*

This interpretation is supported by detailed simulations of the coherent dynamics and of the carrier redistribution processes. Our treatment is based on a generalized Monte Carlo solution of the SBE [13,14], fully accounting for the time dependent scattering rates during the temporal evolution of the nonequilibrium electron distribution. The luminescence spectra are obtained from the calculated distribution functions within the standard Fermi's golden rule approximation [20]. Figures 3(d)–3(f) show the resulting spectra for the same densities as in the experiment. The calculated increase of linewidth of the first luminescence peak with carrier density reproduces our data very well [triangles in Fig. 2(a)]. Furthermore, the spectral widths of the various replicas at a given density which are plotted in Fig. 2(b) (triangles), are nearly identical and in good agreement with the experimental results (squares). It should be noted that the main criteria supporting our interpretation are the identical linewidth of successive luminescence peaks and the much more pronounced density dependence in the coherent model (but not the agreement of the absolute values of the spectral width). This density dependence is related to the details of the *cc* scattering processes. Even if the total *cc* scattering rate is approximately density independent, the decrease in the screening wave vector with decreasing density leads to an increasing number of small-angle scattering processes resulting in a less efficient carrier redistribution and also, as recently pointed out [13], in a less efficient dephasing. The same argument holds for elastic carrier-impurity scattering. With rising density, the efficiency of *cc* scattering for dephasing starts at lower densities than that for electron redistribution. This behavior is due to the fact that the decay of the interband polarization is strongly influenced by hole-hole scattering which is much faster than electron-electron scattering.

In conclusion, we have presented the first experimental evidence that coherent effects play a dominant role for the spectra observed in luminescence experiments. The linewidth of the successively created phonon replicas is nearly constant, a behavior which is explained by a broadening occurring in the generation process. This interpretation is supported by the excellent agreement with the results from a Monte Carlo solution of the semiconductor Bloch equations.

We thank W. Kaiser and S.W. Koch for valuable discussions.

\*Present address: Max-Born-Institut für Nichtlineare Optik und Kurzzeit-spektroskopie, Rudower Chaussee 6, D-12489 Berlin, Germany.

- [1] For a review see J. Shah, *Solid State Electron.* **32**, 1051 (1989).
- [2] W. Z. Lin, R. W. Schoenlein, J. G. Fujimoto, and E. P. Ippen, *IEEE J. Quantum Electron.* **24**, 267 (1988).
- [3] T. Elsaesser, J. Shah, L. Rota, and P. Lugli, *Phys. Rev. Lett.* **66**, 1757 (1991).
- [4] D. N. Mirlin, I. Ja. Karlik, L. P. Nikitin, I. I. Reshina, and V. F. Sapega, *Solid State Commun.* **37**, 757 (1981).
- [5] R. G. Ulbrich, J. A. Kash, and J. C. Tsang, *Phys. Rev. Lett.* **62**, 949 (1989); J. A. Kash, *Phys. Rev. B* **40**, 3455 (1989); **47**, 1221 (1993); J. A. Kash and J. C. Tsang, *Solid State Electron.* **31**, 419 (1988).
- [6] G. Fasol, W. Hackenberg, H. P. Hughes, K. Ploog, E. Bauser, and H. Kano, *Phys. Rev. B* **41**, 1461 (1990).
- [7] D. W. Snoke, W. W. Rühle, Y.-C. Lu, and E. Bauser, *Phys. Rev. Lett.* **68**, 990 (1992); *Phys. Rev. B* **45**, 10979 (1992).
- [8] J. F. Young, N. L. Henry, and P. J. Kelly, *Solid State Electron.* **32**, 1567 (1989).
- [9] M. G. Kane, K. W. Sun, and S. A. Lyon, *Semicond. Sci. Technol.* **9**, 697 (1994).
- [10] P. C. Becker, H. L. Fragnito, C. H. BritoCruz, R. L. Fork, J. E. Cunningham, J. E. Henry, and C. V. Shank, *Phys. Rev. Lett.* **61**, 1647 (1988).
- [11] A. Lohner, K. Rick, P. Leisching, A. Leitenstorfer, T. Elsaesser, T. Kuhn, F. Rossi, and W. Stolz, *Phys. Rev. Lett.* **71**, 77 (1993).
- [12] J. L. Oudar, D. Hulin, A. Migus, A. Antonetti, and F. Alexandre, *Phys. Rev. Lett.* **55**, 2074 (1985).
- [13] F. Rossi, S. Haas, and T. Kuhn, *Phys. Rev. Lett.* **72**, 152 (1994).
- [14] T. Kuhn and F. Rossi, *Phys. Rev. Lett.* **69**, 977 (1992); *Phys. Rev. B* **46**, 7496 (1992).
- [15] D. J. Ashen, P. J. Dean, D. T. J. Hurle, J. B. Mullin, and A. M. White, *J. Chem. Solids* **36**, 1041 (1975).
- [16] For the moderate doping level of the sample, the splitting of the acceptor ground state is less than 4 meV as determined from band-gap related luminescence, i.e., the line shapes of the hot luminescence are not influenced by this effect.
- [17] The pump pulse generates a small fraction of electrons of less than 10% via transitions from the light hole to the conduction band.
- [18] W. P. Dumke, *Phys. Rev.* **132**, 1998 (1963).
- [19] To derive the different linewidths quantitatively, the weak background due to thermalized luminescence is approximated by an exponentially decreasing tail and is subtracted from the spectra.
- [20] It should be noted that this calculation of the spectra is not fully consistent with the coherent approach since also here an additional broadening due to dephasing processes should be taken into account. However, in the present case of a time-integrated measurement, only minor changes are expected.